

Subcycling of particle orbits in variational, geometric electromagnetic particle-in-cell methods

Eero Hirvijoki,¹ Katharina Kormann,^{2,3} and Filippo Zonta¹

¹*Department of Applied Physics, Aalto University,
P.O. Box 11100, 00076 AALTO, Finland**

²*Max-Planck-Institut für Plasmaphysik,
Boltzmannstraße 2, 85748 Garching, Germany*

³*Technische Universität München, Department of Mathematics,
Boltzmannstraße 3, 85748 Garching, Germany*

(Dated: February 26, 2020)

This paper introduces two subcycling algorithms for particle orbits in variational, geometric particle-in-cell methods that address the Vlasov-Maxwell system in magnetized plasmas. The purpose of subcycling is to allow for time steps in the global field solves at or longer than the gyroperiod time scale while sampling the local particle cyclotron orbits accurately. Both algorithms retain the electromagnetic gauge invariance of the discrete action, guaranteeing a local charge conservation law, and the variational approach provides a bounded long-time energy behaviour. In the first algorithm, the global field solves are explicit and the local particle push implicit for each particle individually. The requirement for gauge invariance leads to a peculiar subcycling scheme where the magnetic field is orbit-averaged and the effect of the electric field on the particle orbits is evaluated once during the subcycling period. Numerical tests with this algorithm indicate that artificial oscillations may occur if the electric field impulse on the particles grows large. The oscillations are observed to vanish if orbit-averaging is enforced also for the electric field but then the variational particle push is lost. The second algorithm, a fully implicit one, is proposed to remedy the possible issues of the semi-explicit algorithm. It is observed that both magnetic and electric field can be orbit-averaged, the gauge invariance and consequently the charge conservation retained, while the algorithm remains variational. These requirements, however, appear to require a fully implicit approach. Numerical experiments with and adaptive time-step control for the implicit scheme are left for a future study.

* eero.hirvijoki@gmail.com

I. INTRODUCTION

During the past decade, both understanding and developing of structure-preserving algorithms for simulating plasmas have leaped forward and, to a large extent, this development has been driven by the so-called geometric particle-in-cell (GEMPIC) methods [1–10]—see [11] for a recent review and the exhaustive list of references therein. Based on discretizing either the underlying variational or Hamiltonian structure, GEMPIC algorithms provide long-time fidelity and stability for models with possibly billions of degrees of freedom. This is especially important for kinetic simulations of magnetized fusion plasmas where reaching macroscopic transport at time scales of 10^{-6} s requires a breathtaking number of time steps to resolve the electron cyclotron motion typically appearing at the time scales of 10^{-11} s.

To our knowledge, the GEMPIC methods have so far considered only synchronous integration of particle orbits and electromagnetic fields, whereas the non-GEMPIC methods, that have become the industry standard [12–16], implement so-called subcycling or orbit-averaging of particle orbits out of the box. The only GEMPIC attempt in this direction, reported in [17], is based on an energy-conserving temporal discretization rather than a variational integrator. Especially in simulating multi-component, strongly magnetized plasmas, treating both ions and electrons kinetically, multiple different time scales naturally emerge as the ion and electron cyclotron periods differ by the respective mass ratio. It would be preferable not to restrict the field solve or the ion push to the fastest time scale—the electron cyclotron period—but to allow for subcycling of particle orbits at their naturally occurring frequencies. The absence of this feature from the GEMPIC methods does not need to remain the state of the business, though, and the purpose of this paper is to take the first steps in modifying GEMPIC methods towards fully asynchronous and, in future, possibly temporally adaptive integration.

We introduce two different candidates for implementing subcycling of particle orbits in variational GEMPIC methods. Both algorithms retain the electromagnetic gauge invariance of the discrete action—guaranteeing a local charge conservation law—and the variational approach provides a bounded long-time energy behaviour. Our first algorithm is intended for upgrading the existing variational GEMPIC methods to include subcycling with minimal effort invested in modifications: the global field solves are explicit and the local particle push implicit for each particle individually, just as in the pioneering paper [1]. We anticipate that the scheme could be made fully explicit if rectilinear meshes are exploited as done in [10]. The requirement for gauge invariance, however, leads to a peculiar subcycling scheme where the magnetic field is orbit-averaged and the effect of electric field on the particle orbits is evaluated only once during the subcycling period. Numerical tests with this algorithm indicate that artificial oscillations may occur if the electric field impulse on the particle orbit is too large: in an electrostatically dominated case we observe such modes but in an electromagnetically dominated test we don’t. This behaviour is likely credited to the electric field not being orbit-averaged the same way as the magnetic field is which increases the instantaneous relative impulse from the electric field in comparison to the impulse from the magnetic field. Indeed, the oscillations are observed to vanish if orbit-averaging is enforced also for the electric field but then particle push is no longer variational. It appears that measures more radical than quickly modifying existing schemes are called for.

Our second algorithm is proposed to remedy the issues possibly occurring with the semi-explicit algorithm. Instead of relying on the “summation by parts” trick as in the traditional variational GEMPIC methods, we observe that enabling proper partial integration in the

field-particle interaction term of the discrete action, both magnetic and electric field can be orbit-averaged, the gauge invariance and consequently the charge conservation retained, while the total algorithm remains variational. These choices, however, appear to require a fully implicit approach, in contrast to the clever summation by parts trick that admits explicit field solve. It remains to be seen, if proper orbit-averaging could be performed within the variational framework with explicit schemes. Numerical experiments with and adaptive time-step control for the implicit scheme are left for a future study.

We will begin by briefly recapping the essential elements of a structure-preserving variational discretization of the Vlasov-Maxwell system in Sec. II, and then proceed to presenting the new algorithms. The semi-explicit scheme is introduced in Sec. III together with the numerical experiments indicating the possible oscillation problem and a demonstration that orbit-averaging the electric field removes them. The fully implicit scheme is derived in Sec. IV. Finally, the results are summarized and possible suggestions for future research directions discussed in Sec. V.

II. ELEMENTS OF STRUCTURE-PRESERVING DISCRETIZATION

In this section, we briefly summarize some of the essential building blocks for implementing a variational GEMPIC method for the Vlasov-Maxwell system. For more details, we refer the reader to the excellent papers [1, 9, 10].

Let us assume we have some domain $\Omega \subset \mathbb{R}^3$ and a finite-dimensional discretization of the associated de Rham complex: we expect there to be the sets of scalar and vector valued basis functions $\{W_i^0\}_i$, $\{\mathbf{W}_j^1\}_j$, $\{\mathbf{W}_k^2\}_k$, and $\{W_\ell^3\}_\ell$ such that

$$\nabla W_i^0(\mathbf{x}) = \text{grad}_i^j \mathbf{W}_j^1(\mathbf{x}), \quad (1)$$

$$\nabla \times \mathbf{W}_j^1(\mathbf{x}) = \text{curl}_j^k \mathbf{W}_k^2(\mathbf{x}), \quad (2)$$

$$\nabla \cdot \mathbf{W}_k^2(\mathbf{x}) = \text{div}_k^\ell W_\ell^3(\mathbf{x}), \quad (3)$$

where grad_i^j , curl_j^k , and div_k^ℓ denote the elements of the discrete gradient, curl, and divergence matrices, respectively. Einstein summation over the repeated superscript-subscript index pairs is assumed throughout, and the letters i, j, k, ℓ always refer to the corresponding element spaces as denoted above. A typical way to construct such basis is via the Whitney interpolating functions on simplicial meshes.

Because the basis functions satisfy the de Rham complex, we have that

$$0 = \nabla \times \nabla W_i^0(\mathbf{x}) = \text{grad}_i^j \nabla \times \mathbf{W}_j^1(\mathbf{x}) = \text{grad}_i^j \text{curl}_j^k \mathbf{W}_k^2(\mathbf{x}), \quad (4)$$

$$0 = \nabla \cdot \nabla \times \mathbf{W}_j^1(\mathbf{x}) = \text{curl}_j^k \nabla \cdot \mathbf{W}_k^2(\mathbf{x}) = \text{curl}_j^k \text{div}_k^\ell W_\ell^3(\mathbf{x}), \quad (5)$$

implying the matrix identities $\text{curl}_j^k \text{grad}_i^j = 0$ and $\text{div}_k^\ell \text{curl}_j^k = 0$. The spatial discretizations of the vector and scalar potential are then taken to be

$$\mathbf{A}_{\text{ext}}(\mathbf{x}) = a_{\text{ext}}^j \mathbf{W}_j^1(\mathbf{x}), \quad (6)$$

$$\mathbf{A}(\mathbf{x}, t) = a^j(t) \mathbf{W}_j^1(\mathbf{x}), \quad (7)$$

$$\phi(\mathbf{x}, t) = \phi^i(t) W_i^0(\mathbf{x}), \quad (8)$$

where the subscript "ext" refers to a static, given quantity, and the definitions then imply the following expressions for the finite-dimensional electric and magnetic fields

$$\mathbf{E}(\mathbf{x}, t) = (-\dot{a}^j(t) - \phi^i(t) \text{grad}_i^j) \mathbf{W}_j^1(\mathbf{x}) \equiv e^j(t) \mathbf{W}_j^1(\mathbf{x}), \quad (9)$$

$$\mathbf{B}(\mathbf{x}, t) = a^j(t) \text{curl}_j^k \mathbf{W}_k^2(\mathbf{x}) \equiv b^k(t) \mathbf{W}_k^2(\mathbf{x}). \quad (10)$$

A possible external, fixed magnetic field is naturally denoted by

$$\mathbf{B}_{\text{ext}}(\mathbf{x}) = a_{\text{ext}}^j \text{curl}_j^k \mathbf{W}_k^2(\mathbf{x}) \equiv b_{\text{ext}}^k \mathbf{W}_k^2(\mathbf{x}). \quad (11)$$

The finite-dimensional magnetic field now satisfies the identities

$$\partial_t \mathbf{B}(\mathbf{x}, t) = \dot{a}^j(t) \text{curl}_j^k \mathbf{W}_k^2(\mathbf{x}) = -e^j(t) \nabla \times \mathbf{W}_j^1(\mathbf{x}) = -\nabla \times \mathbf{E}(\mathbf{x}, t), \quad (12)$$

$$\partial_t \nabla \cdot \mathbf{B}(\mathbf{x}, t) = \dot{a}^j \text{curl}_j^k \text{div}_k^\ell \mathbf{W}_\ell^3 = 0, \quad (13)$$

meaning that if the degrees of freedom for \mathbf{B} initially satisfy $b^k \text{div}_k^\ell = 0$, the magnetic field will stay divergence free for all times.

In particle-in-cell methods, the idea is to let marker particles to carry the phase-space density forward in time, starting from a fixed initial density distribution

$$F_0 = \sum_p \delta(\mathbf{x}_0 - \mathbf{x}_p(t_0)) \delta(\mathbf{v}_0 - \dot{\mathbf{x}}_p(t_0)), \quad (14)$$

where $(\mathbf{x}_p(t_0), \dot{\mathbf{x}}_p(t_0))$ are the initial position and velocity coordinates for the marker trajectory $(\mathbf{x}_p(t), \dot{\mathbf{x}}_p(t))$. In practice, every marker should be weighted with a label w_p accounting for the number of real particles the marker represents. Here we have, however, suppressed this factor for notational clarity. From here on, we will also use the tuples $\mathbf{x} = \{\mathbf{x}_p\}_p$, $\dot{\mathbf{x}} = \{\dot{\mathbf{x}}_p\}_p$, $\mathbf{a} = \{a^j\}_j$, $\dot{\mathbf{a}} = \{\dot{a}^j\}_j$, $\mathbf{b} = \{b^k\}_k$, $\mathbf{e} = \{e^j\}_j$, and $\phi = \{\phi^i\}_i$ to group together the degrees of freedom. Especially it is to be understood that ϕ now refers to the tuple of degrees of freedom, not the space-continuous electrostatic potential.

Once the above definitions are cleared, one substitutes them to the Vlasov-Maxwell action functional, performs the integrations over phase space, and obtains a finite-dimensional yet time-continuous action functional

$$S[\mathbf{x}, \dot{\mathbf{x}}, \mathbf{a}, \dot{\mathbf{a}}, \phi] = \int_{t_i}^{t_f} L(\mathbf{x}(t), \dot{\mathbf{x}}(t), \mathbf{a}(t), \dot{\mathbf{a}}(t), \phi(t)) dt, \quad (15)$$

with a new finite-dimensional Lagrangian defined according to

$$\begin{aligned} & L(\mathbf{x}(t), \dot{\mathbf{x}}(t), \mathbf{a}(t), \dot{\mathbf{a}}(t), \phi(t)) \\ &= \frac{\varepsilon_0}{2} e^{j_1} M_{j_1, j_2}^1 e^{j_2} - \frac{\mu_0^{-1}}{2} (b^{k_1} + b_{\text{ext}}^{k_1}) M_{k_1, k_2}^2 (b^{k_2} + b_{\text{ext}}^{k_2}) \\ &+ \sum_p \left[q(a^j + a_{\text{ext}}^j) \mathbf{W}_j^1(\mathbf{x}_p) \cdot \dot{\mathbf{x}}_p - q \phi^i W_i^0(\mathbf{x}_p) + \frac{1}{2} m |\dot{\mathbf{x}}_p|^2 \right]. \end{aligned} \quad (16)$$

where one is to remember the relations $e^j = -\dot{a}^j - \text{grad}_i^j \phi^i$ and $b^k = \text{curl}_j^k a^j$. The finite-element mass matrices in the Lagrangian, related to one-form and two-form element bases,

are defined according to

$$\int_{\Omega} \mathbf{W}_{j_1}^1(\mathbf{x}) \cdot \mathbf{W}_{j_2}^1(\mathbf{x}) d\mathbf{x} = M_{j_1 j_2}^1, \quad (17)$$

$$\int_{\Omega} \mathbf{W}_{k_1}^2(\mathbf{x}) \cdot \mathbf{W}_{k_2}^2(\mathbf{x}) d\mathbf{x} = M_{k_1 k_2}^2. \quad (18)$$

From the perspectives of solving the Vlasov-Maxwell system of equations while respecting the Gauss' law constraints, the electromagnetic gauge invariance turns out to be a key requirement. Let us first perturb $\mathbf{a} \rightarrow \mathbf{a} + \epsilon \delta \mathbf{a}$ and $\phi \rightarrow \phi + \epsilon \delta \phi$ and differentiate the perturbed action with respect to ϵ at $\epsilon = 0$. This computation provides

$$\begin{aligned} & \partial_{\epsilon}|_{\epsilon=0} S[\mathbb{X}, \mathbf{a} + \epsilon \delta \mathbf{a}, \phi + \epsilon \delta \phi] \\ &= - \int_{t_i}^{t_f} \frac{d}{dt} (\delta a^{j_1} \varepsilon_0 M_{j_1, j_2}^1 e^{j_2}) dt + \int_{t_i}^{t_f} \delta a^{j_1} (\varepsilon_0 M_{j_1, j_2}^1 \dot{e}^{j_2} - \mu_0^{-1} \text{curl}_{j_1}^{k_1} M_{k_1, k_2}^2 (b^{k_2} + b_{\text{ext}}^{k_2})) dt \\ & - \int_{t_i}^{t_f} \delta \phi^{i_1} \varepsilon_0 \text{grad}_{i_1}^{j_1} M_{j_1, j_2}^1 e^{j_2} dt + \sum_p \int_{t_i}^{t_f} [q \delta a^j \mathbf{W}_j^1(\mathbf{x}_p) \cdot \dot{\mathbf{x}}_p - q \delta \phi^i W_i^0(\mathbf{x}_p)] dt. \end{aligned} \quad (19)$$

Applying the Hamilton's principle of least action while assuming the perturbations $\delta \mathbf{a}$ and $\delta \phi$ to be arbitrary and to vanish at t_i and t_f , the following Euler-Lagrange equations are obtained

$$\varepsilon_0 M_{j_1, j_2}^1 \dot{e}^{j_2} + \sum_p q \mathbf{W}_{j_1}^1(\mathbf{x}_p) \cdot \dot{\mathbf{x}}_p = \mu_0^{-1} \text{curl}_{j_1}^{k_1} M_{k_1, k_2}^2 (b^{k_2} + b_{\text{ext}}^{k_2}), \quad (20)$$

$$-\varepsilon_0 \text{grad}_{i_1}^{j_1} M_{j_1, j_2}^1 e^{j_2} = \sum_p q W_{i_1}^0(\mathbf{x}_p), \quad (21)$$

corresponding to the finite-dimensional Ampère and Gauss' laws with current density $J_j = \sum_p q \mathbf{W}_j^1(\mathbf{x}_p) \cdot \dot{\mathbf{x}}_p$ and charge density $\varrho_i = \sum_p q W_i^0(\mathbf{x}_p)$. If, however, we choose the very specific forms for the perturbations

$$\delta a^j = \chi^i \text{grad}_i^j, \quad (22)$$

$$\delta \phi^i = -\dot{\chi}^i, \quad (23)$$

requesting that $\chi^i(t_i) = \chi^i(t_f) = 0$, we observe that the differentiation of the transformed action can now be written as

$$\begin{aligned} & \partial_{\epsilon}|_{\epsilon=0} S[\mathbb{X}, a^j + \epsilon \chi^i \text{grad}_i^j, \phi^i - \epsilon \dot{\chi}^i] \\ &= \int_{t_i}^{t_f} \chi^i \left(\text{grad}_i^j \sum_p q \mathbf{W}_j^1(\mathbf{x}_p) \cdot \dot{\mathbf{x}}_p - \frac{d}{dt} \sum_p q W_i^0(\mathbf{x}_p) \right) dt \end{aligned} \quad (24)$$

Because the action also has a strong symmetry with respect to arbitrary χ^i in the sense that

$$S[\mathbb{X}, a^j + \epsilon \chi^i \text{grad}_i^j, \phi^i - \epsilon \dot{\chi}^i] = S[\mathbb{X}, \mathbf{a}, \phi], \quad (25)$$

the differentiation of the transformed action with respect to ϵ has to vanish, providing the finite-dimensional charge conservation law

$$\text{grad}_i^j \sum_p q \mathbf{W}_j^1(\mathbf{x}_p) \cdot \dot{\mathbf{x}}_p - \frac{d}{dt} \sum_p q W_i^0(\mathbf{x}_p) = 0. \quad (26)$$

The importance of this identity lies in the fact that it eliminates the need to solve the Gauss' law: Solving for the electric-field $e^j(t)$ in (20) guarantees such evolution for $e^j(t)$ that it automatically satisfies the Gauss' law (21). It is then a matter of finding a temporal discretization which retains an analog of this property also in the fully discrete case.

III. SUBCYCLING OF PARTICLES WITH AN EXPLICIT FIELD SOLVE

Turning into the details of implementing a subcycling scheme, we first investigate a straightforward modification of existing variational methods. We obtain an algorithm where the particle push is implicit and the field solve explicit. Requesting electromagnetic gauge invariance, the subcycling turns out such that the magnetic field is properly orbit averaged but the effect of the electric field on the particle orbits is evaluated only once during the subcycling period. Numerical tests then suggest that, if the global time step is too long, the resulting large impulse from a single electric kick might lead to artificial oscillations: we observe the phenomenon in an electrostatically dominated test while it is absent in an electromagnetically dominated test. Enforcing orbit-averaging also for the electric field removes the artificial oscillations but we have not found a variational derivation for such particle push.

A. Fully variational, gauge-invariant algorithm

The time integral in the action functional is split into intervals $[t_n, t_{n+1}]$ of equal length Δt in the manner of

$$S[\mathbf{x}(t), \mathbf{a}(t), \phi(t)] = \sum_{n=0}^{N-1} \int_{t_n}^{t_{n+1}} L(\mathbf{x}(t), \dot{\mathbf{x}}(t), \mathbf{a}(t), \dot{\mathbf{a}}(t), \phi(t)) dt = \sum_{n=0}^{N-1} S_{n,n+1}. \quad (27)$$

To obtain discrete update maps for the degrees of freedom $(\mathbf{x}(t), \mathbf{a}(t), \phi(t))$, one assumes some discrete representations for the variable paths in the intervals $t \in [t_n, t_{n+1}]$ and approximates the remaining time integrals somehow. Here, we closely follow the pioneering work [1] but introduce a modification, allowing for subcycling of the particles with \mathcal{V} indicating the number of substeps per global time step Δt .

The discrete action over the time interval $t \in [t_n, t_{n+1}]$ we approximate with the expression

$$\begin{aligned} S_{n,n+1}[\mathbf{x}_n, \mathbf{x}_{n+1/\mathcal{V}}, \mathbf{x}_{n+2/\mathcal{V}}, \dots, \mathbf{x}_{n+1}, \mathbf{a}_n, \mathbf{a}_{n+1}, \phi_n] \\ = \Delta t \frac{\varepsilon_0}{2} e_n^{j_1} M_{j_1, j_2}^1 e_n^{j_2} - \Delta t \frac{\mu_0^{-1}}{2} (b_n^{k_1} + b_{\text{ext}}^{k_1}) M_{k_1 k_2}^2 (b_n^{k_2} + b_{\text{ext}}^{k_2}) \\ + \sum_p \sum_{\nu=1}^{\mathcal{V}} q(a_{n+1}^j + a_{\text{ext}}^j) \int_0^1 \mathbf{W}_j^1(\mathbf{x}_p^{n,\nu}(\tau)) \cdot \frac{d\mathbf{x}_p^{n,\nu}(\tau)}{d\tau} d\tau - \sum_p q\phi_n^i W_i^0(\mathbf{x}_{p,n}) \Delta t \\ + \sum_p \sum_{\nu=1}^{\mathcal{V}} \frac{m}{2} \frac{|\mathbf{x}_{p,n+\nu/\mathcal{V}} - \mathbf{x}_{p,n+(\nu-1)/\mathcal{V}}|^2}{\Delta t/\mathcal{V}}, \end{aligned} \quad (28)$$

where the following abbreviations have been introduced

$$b_n^k = a_n^j \text{curl}_j^k, \quad (29)$$

$$e_n^j = -(a_{n+1}^j - a_n^j)/\Delta t - \phi_n^i \text{grad}_i^j, \quad (30)$$

and $\mathbf{x}_p^{n,\nu}(\tau)$ is a straight trajectory connecting the substeps $(\nu - 1)$ and ν linked to a global step n and defined according to

$$\mathbf{x}_p^{n,\nu}(\tau) = \mathbf{x}_{p,n+(\nu-1)/\mathcal{V}} + \tau(\mathbf{x}_{p,n+\nu/\mathcal{V}} - \mathbf{x}_{p,n+(\nu-1)/\mathcal{V}}). \quad (31)$$

The discrete Euler-Lagrange conditions are derived by perturbing the variables, assuming the perturbations to vanish at the end points in time, and looking for an extrema point of the discrete action. With respect to the perturbations $\mathbf{a}_n \rightarrow \mathbf{a}_n + \epsilon \delta \mathbf{a}_n$, this leads to the equation

$$\partial_\epsilon|_{\epsilon=0} S_{n,n+1}[\mathbf{a}_n + \epsilon \delta \mathbf{a}_n] + \partial_\epsilon|_{\epsilon=0} S_{n-1,n}[\mathbf{a}_n + \epsilon \delta \mathbf{a}_n] = 0, \quad (32)$$

and, when written explicitly, provides the discrete Ampère-Maxwell equation

$$\epsilon_0 M_{j,j_2}^1 \frac{e_n^{j_2} - e_{n-1}^{j_2}}{\Delta t} + J_j^{n-1,n} = \mu_0^{-1} \text{curl}_j^k M_{k,k_2}^2 (b_n^{k_2} + b_{\text{ext}}^{k_2}), \quad (33)$$

with a discrete current density defined according to

$$J_j^{n,n+1} = \sum_p \sum_{\nu=1}^{\mathcal{V}} q \int_0^1 \mathbf{W}_j^1(\mathbf{x}_p^{n,\nu}(\tau)) \cdot \frac{d\mathbf{x}_p^{n,\nu}(\tau)}{d\tau} \frac{d\tau}{\Delta t}. \quad (34)$$

With respect to perturbations $\phi_n \rightarrow \phi_n + \epsilon \delta \phi_n$, the variation of the action leads to

$$\partial_\epsilon|_{\epsilon=0} S_{n,n+1}[\phi_n + \epsilon \delta \phi_n] = 0, \quad (35)$$

which, when written explicitly, corresponds to the discrete Gauss' law

$$\varrho_i^n = -\epsilon_0 \text{grad}_i^j M_{j,j_2}^1 e_n^{j_2}, \quad (36)$$

with the discrete charge density being defined according to

$$\varrho_i^n = \sum_p q W_i^0(\mathbf{x}_{p,n}). \quad (37)$$

With respect to perturbations in the particles' spatial positions, $\mathbf{x}_n \rightarrow \mathbf{x}_n + \epsilon \delta \mathbf{x}_n$ and $\mathbf{x}_{n+\nu/\mathcal{V}} \rightarrow \mathbf{x}_{n+\nu/\mathcal{V}} + \epsilon \delta \mathbf{x}_{n+\nu/\mathcal{V}}$, variation of the action provides

$$\partial_\epsilon|_{\epsilon=0} S_{n,n+1}[\mathbf{x}_n + \epsilon \delta \mathbf{x}_n] + \partial_\epsilon|_{\epsilon=0} S_{n-1,n}[\mathbf{x}_n + \epsilon \delta \mathbf{x}_n] = 0, \quad (38)$$

$$\partial_\epsilon|_{\epsilon=0} S_{n,n+1}[\mathbf{x}_{n+\nu/\mathcal{V}} + \epsilon \delta \mathbf{x}_{n+\nu/\mathcal{V}}] = 0, \quad (39)$$

for each $n = 0, \dots, N - 1$ and $\nu = 1, \dots, \mathcal{V} - 1$. Written explicitly, these correspond to the equations for the indices n

$$\begin{aligned} & m \frac{\mathbf{x}_{p,n+1/\mathcal{V}} - 2\mathbf{x}_{p,n} + \mathbf{x}_{p,n-1/\mathcal{V}}}{(\Delta t/\mathcal{V})^2} \\ &= q \frac{\mathbf{x}_{n+1/\mathcal{V}} - \mathbf{x}_{p,n}}{\Delta t/\mathcal{V}} \times \int_0^1 (1 - \tau)(b_{n+1}^k + b_{\text{ext}}^k) \mathbf{W}_k^2(\mathbf{x}_p^{n,1}(\tau)) d\tau \\ &+ q \frac{\mathbf{x}_{p,n} - \mathbf{x}_{p,n-1/\mathcal{V}}}{\Delta t/\mathcal{V}} \times \int_0^1 \tau(b_n^k + b_{\text{ext}}^k) \mathbf{W}_k^2(\mathbf{x}_p^{n,0}(\tau)) d\tau \\ &+ q \mathcal{V} e_n^j \mathbf{W}_j^1(\mathbf{x}_{p,n}). \end{aligned} \quad (40)$$

and for the indices ν

$$\begin{aligned}
& m \frac{\mathbf{x}_{p,n+(\nu+1)/\mathcal{V}} - 2\mathbf{x}_{p,n+\nu/\mathcal{V}} + \mathbf{x}_{p,n+(\nu-1)/\mathcal{V}}}{(\Delta t/\mathcal{V})^2} \\
&= q \frac{\mathbf{x}_{n+(\nu+1)/\mathcal{V}} - \mathbf{x}_{p,n+\nu/\mathcal{V}}}{\Delta t/\mathcal{V}} \times \int_0^1 (1-\tau)(b_{n+1}^k + b_{\text{ext}}^k) \mathbf{W}_k^2(\mathbf{x}_p^{n,\nu+1}(\tau)) d\tau \\
&+ q \frac{\mathbf{x}_{p,n+\nu/\mathcal{V}} - \mathbf{x}_{p,n+(\nu-1)/\mathcal{V}}}{\Delta t/\mathcal{V}} \times \int_0^1 \tau(b_{n+1}^k + b_{\text{ext}}^k) \mathbf{W}_k^2(\mathbf{x}_p^{n,\nu}(\tau)) d\tau.
\end{aligned} \tag{41}$$

The equations (33), (36), (40), and (41) are to be completed by the discrete Faraday equation that is a direct consequence of the definitions for \mathbf{e}_n , \mathbf{b}_n , namely

$$\frac{b_n^k - b_{n-1}^k}{\Delta t} = -\text{curl}_j^k e_{n-1}^j. \tag{42}$$

The electromagnetic gauge invariance and the discrete charge conservation law are verified in the following manner. Let

$$a_n^j \rightarrow a_n^j + \chi_n^i \text{grad}_i^j, \tag{43}$$

$$\phi_n^i \rightarrow \phi_n^i - \frac{\chi_{n+1}^i - \chi_n^i}{\Delta t}, \tag{44}$$

and the total discrete action (28) will satisfy the strong symmetry condition

$$\begin{aligned}
& \sum_{n=0}^{N-1} S_{n,n+1}(a_n^j + \chi_n^i \text{grad}_i^j, a_{n+1}^j + \chi_{n+1}^i \text{grad}_i^j, \phi_n^i - (\chi_{n+1}^i - \chi_n^i)/\Delta t) \\
&= \sum_{n=0}^{N-1} S_{n,n+1}(\mathbf{a}_n, \mathbf{a}_{n+1}, \phi_n) + \sum_p e_p [\chi_N^i W_i^0(\mathbf{x}_{p,N}) - \chi_0^i W_i^0(\mathbf{x}_{p,0})].
\end{aligned} \tag{45}$$

Differentiating with respect to χ_n at any n such that $n \neq 0$ and $n \neq N$, the right side vanishes identically as it is independent of χ_n , and one finds the discrete charge conservation law

$$\text{grad}_i^j J_j^{n-1,n} - \frac{\varrho_i^n - \varrho_i^{n-1}}{\Delta t} = 0. \tag{46}$$

The significance of this equation is that, if we assume the Gauss' law (36) to hold for $n-1$, the charge conservation and the Ampère equation (33) then imply

$$\varrho_i^n = \varrho_i^{n-1} + \Delta t \text{grad}_i^j J_j^{n-1,n} = -\varepsilon_0 \text{grad}_i^j M_{j,j_2}^1 e_n^{j_2}, \tag{47}$$

meaning that the Gauss' law is automatically satisfied, if it is satisfied initially.

Together the discrete equations provide means of advancing the degrees of freedom \mathbf{x}_n , \mathbf{e}_n , and \mathbf{b}_n in time according to the following strategy

0. Initialize with Gauss law (36) $(\mathbf{b}_0, \mathbf{x}_0) \rightarrow \mathbf{e}_0$ and approximate \mathbf{x}_{-1/N_2}
1. Advance Faraday equation (42): $(\mathbf{e}_n, \mathbf{b}_n) \rightarrow \mathbf{b}_{n+1}$
2. Push markers with (41): $(\mathbf{e}_n, \mathbf{b}_n, \mathbf{b}_{n+1}, \mathbf{x}_{n-1/\mathcal{V}}, \mathbf{x}_n) \rightarrow (\mathbf{x}_{n+1/\mathcal{V}})$
3. Push markers with (40): $(\mathbf{b}_{n+1}, \mathbf{x}_{n+(\nu-1)/\mathcal{V}}, \mathbf{x}_{n+\nu/\mathcal{V}}) \rightarrow (\mathbf{x}_{n+(\nu+1)/\mathcal{V}})$
for each $\nu = 1, \dots, \mathcal{V}-1$
4. Invert Ampère-Maxwell (33): $(\mathbf{e}_n, \mathbf{b}_n, \mathbf{b}_{n+1}, \mathbf{x}_n, \mathbf{x}_{n+1/\mathcal{V}}, \dots, \mathbf{x}_{n+1}) \rightarrow \mathbf{e}_{n+1}$
5. Repeat the steps 1-4 indefinitely

B. Numerical tests

We have implemented the subcycling method within the GEMPIC code in the library SeLaLib [18]. The code is based on a compatible spline-finite-element bases as described in [9]. The major building blocks of our algorithm are very similar to the Hamiltonian splitting used in [9], which we shall use for benchmarking purposes. However, the new subcycling scheme does not build upon a splitting of the kinetic energy into the three components and contains a non-linearity in equations (40) and (41). This non-linearity, however, only couples the three components of the three positions of each particle. This non-linear step can efficiently be solved by a first guess obtained by extrapolation from the old values, followed by one or more updates according to Newton's method. For this, an analytic formula for the derivative matrix can be found and evaluated numerically in the implementation.

1. An electrostatically dominated test case

As a first example of a simulation with strong background magnetic field, we consider a reduced, 1D-2V-dimensional phase space and an initial distribution function of

$$f(x, v_1, v_2, 0) = \frac{1}{2\pi} (1 + 0.1 \cos(0.5x)) \exp\left(-\frac{v_1^2 + v_2^2}{2}\right), \quad (48)$$

set up in a background magnetic field of $B_3(x, 0) = 2\pi 10$. We run the variational subcycling and Hamiltonian splitting algorithms with 32 grid points and 160,000 particles until time 30. In this case, the spatial resolution is given by $\Delta x = 4\pi/32$. Since we split the curl-part in Faraday's and Ampère's law, we get a stability limit of $\Delta t < \Delta x \sqrt{17/42} \approx 0.2498$ (cf. [17, Appendix A2]).

For our choice of the magnetic field, the gyro-period is 0.1. For a time step of $\Delta t = 0.01$ this time scale is resolved well and good results can be obtained even without subcycling. We then increase the global time step to 0.03, 0.06, 0.12, and 0.24. For the Hamiltonian splitting from [9], the simulation runs only stable for $\Delta t = 0.01, 0.03$ and already in the latter case the quality of the result is degraded (see Figure 1a). Figure 1b shows the results of the simulation with our variational subcycling scheme with one step for $\Delta t = 0.01$ and two substeps for all other global time steps. For the nonlinear iteration, we compute the initial guess followed by 2-3 Newton iterations on average to reach an accuracy of 10^{-10} for the individual particle positions. We see that the simulations run stable until the stability limit due to the split in the curl-part of Maxwell's equation. On the other hand, the results show quite high oscillations which we believe to be linked to the way the effect of electric field impulse is evaluated on the particle orbits. Table Ia shows the maximum error in Gauss' law over the whole simulation, which confirms the conservation properties of the subcycling algorithm, while Table Ib shows the error in the conservation of energy, which naturally grows with increasing of the global time step.

The main advantage of the subcycling scheme compared to the Hamiltonian splitting is only the fact that we do not split the trajectories along the three coordinate directions. Increasing the number of subcycles to two (as done in the reported experiments) results in a slight improvement of the results. For more than two subcycles the quality of the results decreases again in the sense that the artificial oscillations begin to grow. This indicates that the subcycling that does not include the orbit-averaging of the electric field does not work well with strong electric fields.

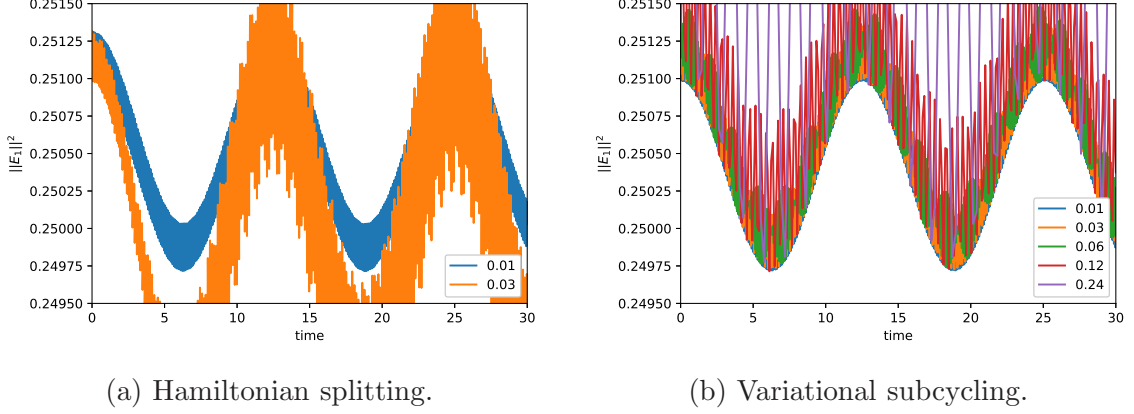


FIG. 1: Electrostatically dominated test case: Time evolution of $\|E_1\|^2$ for the different integrators with various time steps (given in the legends) with $B(x, 0) = 2\pi 10$.

Δt	Ham. splitting	Var. subcycl.
0.01	$1.41 \cdot 10^{-13}$	$1.39 \cdot 10^{-13}$
0.03	$1.40 \cdot 10^{-13}$	$1.38 \cdot 10^{-13}$
0.06	—	$1.39 \cdot 10^{-13}$
0.12	—	$1.39 \cdot 10^{-13}$
0.24	—	$1.40 \cdot 10^{-13}$

(a) Conservation of Gauss' law

Δt	Ham. splitting	Var. subcycl.
0.01	$1.35 \cdot 10^{-1}$	$1.03 \cdot 10^{-4}$
0.03	$8.87 \cdot 10^1$	$3.13 \cdot 10^{-4}$
0.06	—	$8.16 \cdot 10^{-4}$
0.12	—	$2.08 \cdot 10^{-3}$
0.24	—	$6.78 \cdot 10^{-3}$

(b) Conservation of energy

TABLE I: Electrostatic test case: Conservation laws for various propagators and time steps.

2. An electromagnetic test case

As a second example, we look at an electromagnetically dominated test case with initial distribution

$$f(x, v_1, v_2, t = 0) = (1 + 0.1 \cos(kx)) \frac{1}{2\pi\sigma_1\sigma_2} \exp\left(-\frac{1}{2} \left(\frac{v_1^2}{\sigma_1^2} + \frac{v_2^2}{\sigma_2^2}\right)\right), \quad (49)$$

and initial magnetic field $B_0(x) = \beta_1 + \beta_2 \cos(kx)$ on the domain $[0, \frac{2\pi}{k})$. We choose the parameters to be $k = 1.25$, $\sigma_1 = \sqrt{2} \cdot 0.01$, $\sigma_2 = \sqrt{12}\sigma_1$, $\beta_1 = 20\pi$, $\beta_2 = 0.001$. This test case is electromagnetic and a variation of the Weibel instability with a strong background field. The example is a variation of the test problem proposed in [19]. Note that in this case, we do not observe the instability. We run a simulation until time 200 with 32 grid points, 100,000 particles, and spline basis functions of degree 3. The stability limit due to the splitting of the Maxwell's equation is at $\Delta t < (2\pi)/(1.25 \times 32)\sqrt{17/42} \approx 0.09994$ in this case.

Figures 2a and 2b show the electric energy for simulations with subcycling and the variational splitting, respectively, for various time steps. In this test case, both the Hamiltonian splitting and the subcycling scheme yield stable results until the stability limit of the Maxwell part is reached. However, the quality of the results is considerably better with the subcycling scheme for the larger time steps of 0.06 and 0.09. We report here the results with 1

($\Delta t = 0.01$), 2 ($\Delta t = 0.03$), 4 ($\Delta t = 0.06, 0.09$) substeps per one global time step. We note that we did not further increase the number of subcycles when increasing the time step from 0.06 to 0.09, since no improvement in accuracy has been observed beyond the 4 subcycles. The number of Newton updates needed to reach the convergence down to a tolerance of 10^{-10} is between 1 and 2 on average in all four simulations. Table IIa shows the maximum error in Gauss' law over the whole simulation, which again confirms the conservation properties of the subcycling algorithm. Table IIb shows the error in the conservation of energy, which again grows with increasing the global time step.

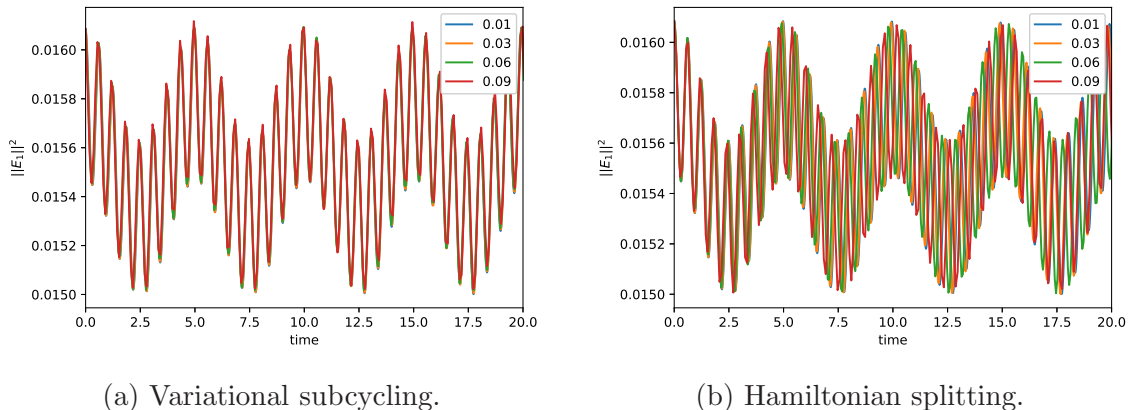


FIG. 2: Electromagnetically dominated test case: Time evolution of $\|E_1\|^2$ for the different integrators with various time steps (given in the legends) with $B(x, 0) = 10 + 0.001 \cos(kx)$.

Δt	Ham. splitting	Var. subcycl.
0.01	$1.52 \cdot 10^{-14}$	$1.50 \cdot 10^{-14}$
0.03	$1.50 \cdot 10^{-14}$	$1.50 \cdot 10^{-14}$
0.06	$1.53 \cdot 10^{-14}$	$1.51 \cdot 10^{-14}$
0.09	$1.48 \cdot 10^{-14}$	$1.48 \cdot 10^{-14}$

(a) Conservation of Gauss' law

Δt	Ham. splitting	Var. subcycl.
0.01	$2.80 \cdot 10^{-5}$	$1.74 \cdot 10^{-5}$
0.03	$2.52 \cdot 10^{-4}$	$5.58 \cdot 10^{-5}$
0.06	$9.98 \cdot 10^{-4}$	$1.23 \cdot 10^{-4}$
0.09	$2.21 \cdot 10^{-3}$	$2.00 \cdot 10^{-4}$

(b) Conservation of energy

TABLE II: Electromagnetic test case: Conservation laws for various propagators and time steps.

Notice that in this electromagnetic case, we do not observe any spurious oscillations when introducing subcycling of particle orbits. This is likely due to the impulse from the electric-field push remaining small enough, even when it is evaluated only once per subcycle. This is supported by noticing that the electric energy in this test case is an order of magnitude lower than in the electrostatically dominated case.

C. Enforcing orbit-averaging

To investigate whether the root cause for the possible numerical oscillations is indeed in the way the electric field is evaluated in particle orbits, we will now enforce orbit-averaging

also for the electric-field contribution. For the indices n , we will use the following modified particle push

$$\begin{aligned}
& m \frac{\mathbf{x}_{p,n+1/\nu} - 2\mathbf{x}_{p,n} + \mathbf{x}_{p,n-1/\nu}}{(\Delta t/\nu)^2} \\
&= q \frac{\mathbf{x}_{n+1/\nu} - \mathbf{x}_{p,n}}{\Delta t/\nu} \times \int_0^1 (1-\tau)(b_{n+1}^k + b_{\text{ext}}^k) \mathbf{W}_k^2(\mathbf{x}_p^{n,1}(\tau)) d\tau \\
&+ q \frac{\mathbf{x}_{p,n} - \mathbf{x}_{p,n-1/\nu}}{\Delta t/\nu} \times \int_0^1 \tau(b_n^k + b_{\text{ext}}^k) \mathbf{W}_k^2(\mathbf{x}_p^{n,0}(\tau)) d\tau \\
&+ q e_n^j \mathbf{W}_j^1(\mathbf{x}_{p,n}),
\end{aligned} \tag{50}$$

and similarly for the indices ν

$$\begin{aligned}
& m \frac{\mathbf{x}_{p,n+(\nu+1)/\nu} - 2\mathbf{x}_{p,n+\nu/\nu} + \mathbf{x}_{p,n+(\nu-1)/\nu}}{(\Delta t/\nu)^2} \\
&= q \frac{\mathbf{x}_{n+(\nu+1)/\nu} - \mathbf{x}_{p,n+\nu/\nu}}{\Delta t/\nu} \times \int_0^1 (1-\tau)(b_{n+1}^k + b_{\text{ext}}^k) \mathbf{W}_k^2(\mathbf{x}_p^{n,\nu+1}(\tau)) d\tau \\
&+ q \frac{\mathbf{x}_{p,n+\nu/\nu} - \mathbf{x}_{p,n+(\nu-1)/\nu}}{\Delta t/\nu} \times \int_0^1 \tau(b_{n+1}^k + b_{\text{ext}}^k) \mathbf{W}_k^2(\mathbf{x}_p^{n,\nu}(\tau)) d\tau \\
&+ q e_n^j \mathbf{W}_j^1(\mathbf{x}_{p,n+\nu/\nu}).
\end{aligned} \tag{51}$$

We stress that this algorithm is not derived from an action principle and is not expected to provide bounded long-time energy behaviour like the variational schemes. For the field equations, we use the Ampère and Gauss' law as described previously for they satisfy a charge conservation law regardless of how the particle orbits are sampled.

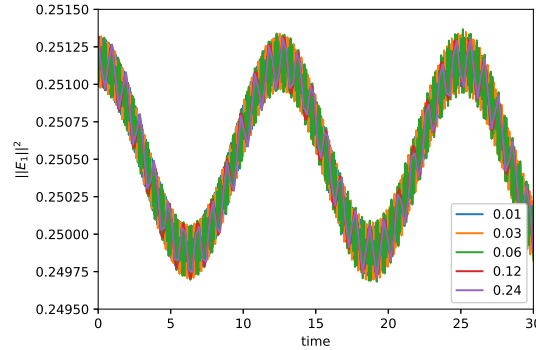


FIG. 3: Electrostatically dominated test case: Time evolution of $\|E_1\|^2$ for the subcycling algorithm with enforced electric-field orbit-averaging for various time steps (given in the legends).

We then repeated the numerical tests from the previous section using the above particle equations. For the electrostatically dominated test case, Figure 3 shows the evolution of the first component of the electric energy as a function of time with the new algorithm and the number of subcycles increased to 4 ($\Delta t = 0.06$), 8 ($\Delta t = 0.12$), and 16 ($\Delta t = 0.24$). We observe that the artificial oscillations are indeed gone. The behaviour of the solution remains better even if the global step size is increased beyond the cyclotron period, which is our ultimate goal. In the electromagnetically dominated test case, we don't see further improvements from the original algorithm for it worked well.

IV. AN IMPLICIT SCHEME WITH FULL ORBIT-AVERAGING AND ELECTROMAGNETIC GAUGE INVARIANCE

To find a variational scheme that would succeed in fully orbit-averaging the particles trajectories, we suggest a temporal discretization that appears to lead to a fully implicit scheme. Essentially, we have learned that the key likely is in handling the interaction term in the action integral in a manner that properly allows one to perform integration by parts in time, instead of the summation by parts trick that works nicely without subcycling and apparently with certain limitations together with subcycling as described in Sec. III. It remains to be seen whether an explicit field-solve strategy, succeeding in both proper orbit-averaging and electromagnetic gauge invariance, is possible.

A. Polyline particle trajectories

We will now assume that the particle trajectories form a polyline between different time instances and shall respect this assumption in the discretization. We partition the interval $[t_i, t_f]$ into multiple arbitrary intervals $t_i = t_0 < t_1 < \dots < t_{n-1} < t_n < t_{n+1} < \dots < t_f$ and during each interval, the particle trajectory is expressed as

$$\mathbf{x}_p^{n,n+1}(t) = \mathbf{x}_{p,n} + \frac{t - t_n}{t_{n+1} - t_n}(\mathbf{x}_{p,n+1} - \mathbf{x}_{p,n}), \quad (52)$$

$$\dot{\mathbf{x}}_p^{n,n+1}(t) = \frac{\mathbf{x}_{p,n+1} - \mathbf{x}_{p,n}}{t_{n+1} - t_n}, \quad (53)$$

making sure that the time derivative is consistent with the trajectory. Substituting these expressions into the action, we find the following particle-relevant contribution over the interval $[t_n, t_{n+1}]$

$$\begin{aligned} & S_{n,n+1}^p[\mathbf{a}(t), \phi(t), \mathbf{x}_n, \mathbf{x}_{n+1}] \\ &= q \int_{t_n}^{t_{n+1}} ((a^j(t) + a_{\text{ext}}^j) \mathbf{W}_j^1(\mathbf{x}_p^{n,n+1}(t)) \cdot \dot{\mathbf{x}}_p^{n,n+1}(t) - \phi^i(t) W_i^0(\mathbf{x}_p^{n,n+1}(t))) dt \\ &+ \frac{1}{2} m \int_{t_n}^{t_{n+1}} |\dot{\mathbf{x}}_p^{n,n+1}|^2 dt. \end{aligned} \quad (54)$$

Perturbing the particle polylines into $\mathbf{x}_n + \epsilon \delta \mathbf{x}_n$ and minimizing the action with respect to the variations in the particle positions, we obtain the following discrete Euler-Lagrange condition for each particle

$$\partial_{\epsilon}|_{\epsilon=0} S_{n,n+1}^p[\mathbf{x}_{p,n} + \epsilon \delta \mathbf{x}_{p,n}] + \partial_{\epsilon}|_{\epsilon=0} S_{n-1,n}^p[\mathbf{x}_{p,n} + \epsilon \delta \mathbf{x}_{p,n}] = 0. \quad (55)$$

Written explicitly, this corresponds to the following discrete Euler-Lagrange condition

$$\begin{aligned}
0 = & q \frac{\mathbf{x}_{p,n+1} - \mathbf{x}_{p,n}}{t_{n+1} - t_n} \times \int_{t_n}^{t_{n+1}} (b^k(t) + b_{\text{ext}}^k) \left(1 - \frac{t-t_n}{t_{n+1}-t_n}\right) \mathbf{W}_k^2(\mathbf{x}_p^{n,n+1}(t)) dt \\
& + q \frac{\mathbf{x}_{p,n} - \mathbf{x}_{p,n-1}}{t_n - t_{n-1}} \times \int_{t_{n-1}}^{t_n} (b^k(t) + b_{\text{ext}}^k) \frac{t-t_{n-1}}{t_n-t_{n-1}} \mathbf{W}_k^2(\mathbf{x}_p^{n-1,n}(t)) dt \\
& + q \int_{t_{n-1}}^{t_n} e^j(t) \frac{t-t_{n-1}}{t_n-t_{n-1}} \mathbf{W}_j^1(\mathbf{x}_p^{n-1,n}(t)) dt \\
& + q \int_{t_n}^{t_{n+1}} e^j(t) \left(1 - \frac{t-t_n}{t_{n+1}-t_n}\right) \mathbf{W}_j^1(\mathbf{x}_p^{n,n+1}(t)) dt \\
& + m \frac{\mathbf{x}_{p,n} - \mathbf{x}_{p,n-1}}{t_n - t_{n-1}} - m \frac{\mathbf{x}_{p,n+1} - \mathbf{x}_{p,n}}{t_{n+1} - t_n}, \tag{56}
\end{aligned}$$

where we have associated $e^j(t) = -\dot{a}^j(t) - \phi^i(t) \text{grad}_i^j$.

In deriving the expression (56), it was necessary to request time-continuity for $a^j(t)$ but not for $\phi^i(t)$. Hence we can still imagine a piece-wise time-constant electric field $e^j(t) = -\dot{a}^j(t) - \text{grad}_i^j \phi^i(t)$. However, the magnetic field $b^k(t)$ has to be at least piece-wise linear in time for it needs to be compatible with $a^j(t)$.

B. Polyline $a(t)$ and piece-wise constant $\phi(t)$

Next we partition the interval $[t_i, t_f]$ according to $t_i = t_0 < t_1 < \dots < t_{\nu-1} < t_\nu < t_{\nu+1} < \dots < t_f$, again with arbitrary intervals. During each interval $[t_\nu, t_{\nu+1}]$ we assume the following behaviour for the electromagnetic degrees of freedom

$$a_{\nu,\nu+1}^j(t) = a_\nu^j + \frac{t - t_\nu}{t_{\nu+1} - t_\nu} (a_{\nu+1}^j - a_\nu^j), \tag{57}$$

$$\phi_{\nu,\nu+1}^i(t) = \phi_\nu^i, \tag{58}$$

which implies that we can define the electric and magnetic field during the interval directly via the relations

$$b_{\nu,\nu+1}^k(t) = a_{\nu,\nu+1}^j(t) \text{curl}_j^k \equiv b_\nu^k + \frac{t - t_\nu}{t_{\nu+1} - t_\nu} (b_{\nu+1}^k - b_\nu^k), \tag{59}$$

$$e_{\nu,\nu+1}^j(t) = -\frac{a_{\nu+1}^j - a_\nu^j}{t_{\nu+1} - t_\nu} - \phi_\nu^i \text{grad}_i^j \equiv e_\nu^j. \tag{60}$$

The above discretizations satisfy the requirements for the magnetic field to be at least time-continuous and the electric field at least piece-wise constant, thus being compatible with Eq. (56). The discretization also implies a convenient form for the discrete Faraday law

$$\frac{b_{\nu+1}^k - b_\nu^k}{t_{\nu+1} - t_\nu} = -e_\nu^j \text{curl}_j^k. \tag{61}$$

Substituting these expressions into the action, we find the following electromagnetic-relevant contribution over the interval $[t_\nu, t_{\nu+1}]$

$$\begin{aligned}
& S_{\nu,\nu+1}^{\text{EM}}[\mathbf{a}_\nu, \mathbf{a}_{\nu+1}, \phi_\nu, \mathbf{x}(t)] \\
&= \frac{\varepsilon_0}{2} \int_{t_\nu}^{t_{\nu+1}} (-\dot{a}_{\nu,\nu+1}^{j_1}(t) - \phi_\nu^{i_1} \text{grad}_{i_1}^{j_1}) M_{j_1,j_2}^1 (-\dot{a}_{\nu,\nu+1}^{j_2}(t) - \phi_\nu^{i_2} \text{grad}_{i_2}^{j_2}) dt \\
&- \frac{\mu_0^{-1}}{2} \int_{t_\nu}^{t_{\nu+1}} (a_{\nu,\nu+1}^{j_1}(t) + a_{\text{ext}}^{j_1}) \text{curl}_{j_1}^{k_1} M_{k_1,k_2}^2 \text{curl}_{j_2}^{k_2} (a_{\nu,\nu+1}^{j_2}(t) + a_{\text{ext}}^{j_2}) dt \\
&+ q \sum_p \int_{t_\nu}^{t_{\nu+1}} [(a_{\nu,\nu+1}^j(t) + a_{\text{ext}}^j) \mathbf{W}_j^1(\mathbf{x}_p(t)) \cdot \dot{\mathbf{x}}_p(t) - \phi_\nu^i W_i^0(\mathbf{x}_p(t))] dt. \tag{62}
\end{aligned}$$

Next we perturb the degrees of freedom for the vector potential into $\mathbf{a}_\nu + \epsilon \delta \mathbf{a}_\nu$ and minimize the action with respect to the variations $\delta \mathbf{a}_\nu$. This provides the discrete Euler-Lagrange equation

$$\partial_\epsilon|_{\epsilon=0} S_{\nu,\nu+1}^{\text{EM}}[\mathbf{a}_\nu + \epsilon \delta \mathbf{a}_\nu] + \partial_\epsilon|_{\epsilon=0} S_{\nu-1,\nu}^{\text{EM}}[\mathbf{a}_\nu + \epsilon \delta \mathbf{a}_\nu] = 0, \tag{63}$$

and explicitly it provides the following discrete Ampère equation

$$\begin{aligned}
& \varepsilon_0 M_{j_1,j_2}^1 (e_\nu^{j_2} - e_{\nu-1}^{j_2}) + J_{j_+}^{\nu,\nu+1} (t_{\nu+1} - t_\nu) + J_{j_-}^{\nu-1,\nu} (t_\nu - t_{\nu-1}) \\
&= \mu_0^{-1} \text{curl}_{j_1}^{k_1} M_{k_1,k_2}^2 \left[\frac{1}{6} (b_{\nu+1}^{k_2} - b_\nu^{k_2}) + \frac{1}{2} (b_\nu^{k_2} + b_{\text{ext}}^{k_2}) \right] (t_{\nu+1} - t_\nu) \\
&+ \mu_0^{-1} \text{curl}_{j_1}^{k_1} M_{k_1,k_2}^2 \left[\frac{1}{3} (b_\nu^{k_2} - b_{\nu-1}^{k_2}) + \frac{1}{2} (b_{\nu-1}^{k_2} + b_{\text{ext}}^{k_2}) \right] (t_\nu - t_{\nu-1}) \tag{64}
\end{aligned}$$

where the discrete current densities are defined via the relations

$$J_{j_+}^{\nu,\nu+1} = q \sum_p \int_{t_\nu}^{t_{\nu+1}} \left(1 - \frac{t-t_\nu}{t_{\nu+1}-t_\nu}\right) \mathbf{W}_{j_1}^1(\mathbf{x}_p(t)) \cdot \dot{\mathbf{x}}_p(t) \frac{dt}{t_{\nu+1} - t_\nu} \tag{65}$$

$$J_{j_-}^{\nu,\nu+1} = q \sum_p \int_{t_\nu}^{t_{\nu+1}} \frac{t-t_\nu}{t_{\nu+1}-t_\nu} \mathbf{W}_{j_1}^1(\mathbf{x}_p(t)) \cdot \dot{\mathbf{x}}_p(t) \frac{dt}{t_{\nu+1} - t_\nu}. \tag{66}$$

Note that in deriving the expression (64), it is enough to require continuity from $\mathbf{x}_p(t)$, while the corresponding $\dot{\mathbf{x}}_p(t)$ can be piece-wise constant. Hence this Ampère equation and the equation for the particle motion (56) are fully compatible with each other. One only has to account for the fact that the instances t_ν and t_n do not necessarily coincide. Also note that if the time steps are assumed of equal length, say Δt , then the rather odd looking term in (64) becomes

$$\begin{aligned}
& \left(\frac{1}{6} (b_{\nu+1} - b_\nu) + \frac{1}{2} (b_\nu + b_{\text{ext}}) \right) (t_{\nu+1} - t_\nu) \\
&+ \left(\frac{1}{3} (b_\nu - b_{\nu-1}) + \frac{1}{2} (b_{\nu-1} + b_{\text{ext}}) \right) (t_\nu - t_{\nu-1}) \\
&= \left(\frac{2}{3} b_\nu + \frac{1}{6} b_{\nu+1} + \frac{1}{6} b_{\nu-1} + b_{\text{ext}} \right) \Delta t. \tag{67}
\end{aligned}$$

Finally perturbing the degrees for the scalar potential to $\phi_\nu + \epsilon \delta \phi_\nu$ and extremizing the action with respect to arbitrary variations $\delta \phi_\nu$ according to

$$\partial_\epsilon|_{\epsilon=0} S_{\nu,\nu+1}^{\text{EM}}[\phi_\nu + \epsilon \delta \phi_\nu] = 0 \tag{68}$$

provides the discrete Gauss' law

$$\varrho_i^{\nu,\nu+1} = -\varepsilon_0 \text{grad}_i^j M_{j,j_2}^1 e_\nu^{j_2}, \quad (69)$$

where the discrete charge density is defined as

$$\varrho_i^{\nu,\nu+1} = q \sum_p \int_{t_\nu}^{t_{\nu+1}} W_i^0(\mathbf{x}_p(t)) \frac{dt}{t_{\nu+1} - t_\nu}. \quad (70)$$

C. Gauge invariance and the charge-conservation law

To demonstrate that the Gauss' law (69) serves only as an initial condition and that it is enough to advance the electric field degrees of freedom via the discrete Ampère equation (64), we start from the electromagnetic gauge invariance.

We define a gauge transformation with a function

$$\chi_{\nu,\nu+1}^i(t) = \chi_\nu^i + \frac{t - t_\nu}{t_{\nu+1} - t_\nu} (\chi_{\nu+1}^i - \chi_\nu^i), \quad (71)$$

and change the discrete vector and scalar potentials according to

$$a_{\nu,\nu+1}^j(t) \rightarrow a_{\nu,\nu+1}^j(t) + \chi_{\nu,\nu+1}^i(t) \text{grad}_i^j, \quad (72)$$

$$\phi_{\nu,\nu+1}^i(t) \rightarrow \phi_{\nu,\nu+1}^i(t) - \dot{\chi}_{\nu,\nu+1}^i(t). \quad (73)$$

The discrete electric and magnetic field are trivially unchanged under these substitutions and the relevant part of the action then satisfies

$$\begin{aligned} & \sum_{\nu=0}^{N_\nu-1} S_{\nu,\nu+1}^{\text{EM}} [a_\nu^j + \text{grad}_i^j \chi_\nu^i, a_{\nu+1} + \text{grad}_i^j \chi_{\nu+1}^i, \phi_\nu - (\chi_{\nu+1}^i - \chi_\nu^i)/(t_{\nu+1} - t_\nu), \mathfrak{x}(t)] \\ &= \sum_{\nu=0}^{N_\nu-1} S_{\nu,\nu+1}^{\text{EM}} [a_\nu^j, a_{\nu+1}, \phi_\nu, \mathfrak{x}(t)] + q \sum_p [\chi_{N_\nu}^i W_i^0(\mathbf{x}_p(t_f)) - \chi_0^i W_i^0(\mathbf{x}_p(t_i))]. \end{aligned} \quad (74)$$

Proceeding as previously, i.e., differentiating the above relation with respect to χ_ν^i for arbitrary $\nu \in [1, N_\nu - 1]$, provides the discrete charge conservation law

$$\text{grad}_i^j [J_{j+}^{\nu,\nu+1}(t_{\nu+1} - t_\nu) + J_{j-}^{\nu-1,\nu}(t_\nu - t_{\nu-1})] - (\varrho_i^{\nu,\nu+1} - \varrho_i^{\nu-1,\nu}) = 0, \quad (75)$$

where the current and charge densities are as defined in the equations (65), (66), and (70).

Assuming the discrete Gauss' law (69) to hold for $\nu - 1$, it is then a straightforward task to use the Ampère equation (64) together with the charge conservation law (75) to obtain

$$\varrho_i^{\nu,\nu+1} = \varrho_i^{\nu-1,\nu} - \text{grad}_i^j [J_{j+}^{\nu,\nu+1}(t_{\nu+1} - t_\nu) + J_{j-}^{\nu-1,\nu}(t_\nu - t_{\nu-1})] = -\varepsilon_0 \text{grad}_i^j M_{j,j_2}^1 e_\nu^{j_2}. \quad (76)$$

This means that if the Gauss' law holds initially, it will be satisfied for all times when we solve the electric field from the Ampère equation. This result is fully analogous with the one we obtained for the algorithm with an explicit field solve in Sec. III.

V. SUMMARY

In this paper, we have introduced two possible subcycling algorithms for variational GEMPIC methods addressing the Vlasov-Maxwell system in magnetized plasmas. The first one is a straightforward upgrade of the existing variational GEMPIC methods, especially of the one given in [1]. The algorithm was tested both in electrostatically and electromagnetically dominated cases. The tests revealed that the resulting, rather peculiar subcycling scheme—magnetic field is properly orbit-averaged but the electric-field impulse evaluated only once per the subcycling period—may result in artificial oscillations if the electric field impulse is too strong in relation to the magnetic field impulse. This was verified by enforcing the electric-field orbit-averaging which removed the spurious oscillations but simultaneously broke the charge conservation. We have performed also low-resolution 3-D simulations and the results remain qualitatively the same.

Our second algorithm is aimed at solving the possible limitations of the first algorithm. Instead of relying on the "summation-by-parts trick", which is the corner stone of the existing electromagnetically gauge invariant variational GEMPIC methods, we considered the possibility of performing genuine integration by parts instead. This lead us to suggest an algorithm where the orbit-averaging is done properly for both the electric and magnetic impulse and which retains the gauge invariance and hence the algebraic charge-conservation law. The trade-off is, however, that the algorithm becomes fully implicit and it appears difficult to find an explicit one: It is necessary to treat the electromagnetic potential as being time-continuous for the sake of performing partial integrations and this couples the degrees of freedom for the vector potential from two different global time instances to all of the substeps in between the instances and ultimately results in an implicit scheme. It remains to be seen whether an explicit subcycling scheme with proper orbit-averaging of both electric and magnetic impulses and an algebraic charge conservation is possible. On the other hand, implicit schemes may avoid the strict CFL-condition.

In the future, we aim to investigate the possibility of expanding further, to admit adaptive temporal integration. Such algorithm would be ideal from the perspectives that the guiding magnetic field in fusion devices may vary spatially. For example in ITER, the inboard magnetic field strength will be approximately 7 T while the outboard side will be at 4 T.

ACKNOWLEDGMENTS

Financial support for the work of E.H. and F.Z. was provided by the Academy of Finland grant Nos. 315278 and 320058. Work of K.K. has been carried out within the framework of the EUROfusion Consortium and has received funding from the Euratom research and training programme 2014–2018 and 2019–2020 under grant agreement No 633053. The views and opinions expressed herein do not necessarily reflect those of the European Commission, Academy of Finland, or Aalto University.

-
- [1] J. Squire, H. Qin, and W. M. Tang, "Geometric integration of the Vlasov-Maxwell system with a variational particle-in-cell scheme," *Physics of Plasmas* **19**, 084501 (2012), [arXiv:1401.6723](https://arxiv.org/abs/1401.6723).

- [2] E. G. Evstatiev and B. A. Shadwick, “Variational formulation of particle algorithms for kinetic plasma simulations,” *Journal of Computational Physics* **245**, 376–398 (2013), [arXiv:1210.3743](#).
- [3] B. A. Shadwick, A. B. Stamm, and E. G. Evstatiev, “Variational formulation of macro-particle plasma simulation algorithms,” *Physics of Plasmas* **21**, 055708 (2014).
- [4] A. B. Stamm, B. A. Shadwick, and E. G. Evstatiev, “Variational Formulation of Macroparticle Models for Electromagnetic Plasma Simulations,” *IEEE Transactions on Plasma Science* **42**, 1747–1758 (2014).
- [5] Jianyuan Xiao, Hong Qin, Jian Liu, Yang He, Ruili Zhang, and Yajuan Sun, “Explicit high-order non-canonical symplectic particle-in-cell algorithms for Vlasov-Maxwell systems,” *Physics of Plasmas* **22**, 112504 (2015), [arXiv:1510.06972](#).
- [6] Yang He, Hong Qin, Yajuan Sun, Jianyuan Xiao, Ruili Zhang, and Jian Liu, “Hamiltonian time integrators for Vlasov-Maxwell equations,” *Physics of Plasmas* **22**, 124503 (2015), [arXiv:1505.06076](#).
- [7] Hong Qin, Jian Liu, Jianyuan Xiao, Ruili Zhang, Yang He, Yulei Wang, Yajuan Sun, Joshua W. Burby, Leland Ellison, and Yao Zhou, “Canonical symplectic particle-in-cell method for long-term large-scale simulations of the Vlasov-Maxwell equations,” *Nuclear Fusion* **56**, 014001 (2016), [arXiv:1503.08334](#).
- [8] Jianyuan Xiao, Hong Qin, Philip J. Morrison, Jian Liu, Zhi Yu, Ruili Zhang, and Yang He, “Explicit high-order noncanonical symplectic algorithms for ideal two-fluid systems,” *Physics of Plasmas* **23**, 112107 (2016), [arXiv:1606.07005](#).
- [9] Michael Kraus, Katharina Kormann, Philip J. Morrison, and Eric Sonnendrücker, “GEMPIC: geometric electromagnetic particle-in-cell methods,” *Journal of Plasma Physics* **83**, 905830401 (2017), [arXiv:1609.03053](#).
- [10] Jianyuan Xiao, Hong Qin, and Jian Liu, “Structure-preserving geometric particle-in-cell methods for Vlasov-Maxwell systems,” *Plasma Science and Technology* **20**, 110501 (2018), [arXiv:1804.08823](#).
- [11] P. J. Morrison, “Structure and structure-preserving algorithms for plasma physics,” *Physics of Plasmas* **24**, 055502 (2017), [arXiv:1612.06734](#).
- [12] G Chen, Luis Chacón, and D C Barnes, “An energy- and charge-conserving, implicit, electrostatic particle-in-cell algorithm,” *Journal of Computational Physics* **230**, 7018–7036 (2011).
- [13] Luis Chacón, G Chen, and D C Barnes, “A charge- and energy-conserving implicit, electrostatic particle-in-cell algorithm on mapped computational meshes,” *Journal of Computational Physics* **233**, 1–16 (2013).
- [14] G Chen and Luis Chacón, “An energy- and charge-conserving, nonlinearly implicit, electromagnetic 1D–3V Vlasov–Darwin particle-in-cell algorithm,” *Computer Physics Communications* **185**, 2391–2402 (2014).
- [15] Luis Chacón and G Chen, “A curvilinear, fully implicit, conservative electromagnetic PIC algorithm in multiple dimensions,” *Journal of Computational Physics* **316**, 578–597 (2016).
- [16] Guangye Chen, Luis Chacón, Lin Yin, Brian J. Albright, David J. Stark, and Robert F. Bird, “A semi-implicit, energy- and charge-conserving particle-in-cell algorithm for the relativistic Vlasov-Maxwell equations,” *arXiv e-prints* (2019), [arXiv:1903.01565](#).
- [17] Katharina Kormann and Eric Sonnendrücker, “Energy-conserving time propagation for a geometric particle-in-cell Vlasov–Maxwell solver,” (2019), [arXiv:1910.04000](#).
- [18] “Selalib,” <http://selalib.gforge.inria.fr/>.
- [19] Joackim Bernier, Fernando Casas, and Nicolas Crouseilles, “Splitting methods for rotations: application to vlasov equations,” (2019), working paper or preprint.